PROCEEDINGS, Thirty-Ninth Workshop on Geothermal Reservoir Engineering
Stanford University, Stanford, California, February 24-26, 2014
SGP-TR-202

Implications of geology, structure and tectonic setting for heat extraction on the Eastern Snake River Plain

Alex Moody[1] and Mitchell A. Plummer[2]

[1]Dept. of Geological Sciences, University of Idaho, 875 Perimeter Drive, MS 3022, Moscow, ID 83844

[2]Energy Resources Recovery and Sustainability Dept., Idaho National Laboratory, 2525 Fremont Ave., Idaho Falls, ID 83415

[1]mood1523@vandals.uidaho.edu, [2]mitchell.plummer@inl.gov

Keywords: Enhanced Geothermal System, Snake River Plain, heat extraction modeling

ABSTRACT

Typically, high-temperature geothermal systems are found in regions of high geothermal gradients and strain rates that are host to an adequate and accessible groundwater supply to be used as a medium for heat exchange with the surrounding rock matrix. In some regions such as older collapsed calderas, there are reservoirs with extensive amounts of heat resources that lack either the permeability and hydraulic connectivity or the deep circulating waters necessary for traditional geothermal power production. The Snake River Plain is one such area with high geothermal gradients that was unfavorable in the past due to limitations in in-situ groundwater and proper circulation. As more attention is focused on the region with the advancement of Engineered Geothermal Systems (EGS), the high heat flow beneath the extensive Snake River Plain Aquifer can be reassessed in terms of potential thermal energy available. While enhancement of the reservoir is likely to increase the efficiency of the geothermal system, preliminary calculations of extractable heat energy based on the remote state of stress and structural context will inform where the optimal geothermal reservoirs are. Heat extraction of the Snake River Plain must consider the large-volume rhyolitic volcanism and caldera formation that defines the structure, lithologies and therefore the permeability of a given site. Given these criteria, we use a semi-analytical heat transfer models in the context of in-place geologic structures and suggest a tentative fracturing plan for augmenting the permeability and connectivity of the reservoir, thereby increasing the efficiency of heat exchange by induced fluid flow.

1.INTRODUCTION

With emerging EGS technologies and a resurgence in the study of the deep subsurface beneath the Snake River Plain (SRP), the geothermal resource potential of the region is being reassessed. Likely sites for a geothermal power plant would be located near caldera ring faults where there are pre-existing areas of high fracture density. Having forming from the same mantle heat source as the Yellowstone Plateau (YP), the inferred buried calderas have sealed faults due to the cooling of hydrothermal waters and cessation of significant volcanic activity, making it ideal for reservoir stimulation.

We present here a brief review of what is known about the geology, heat flow, stress state, fracture distribution, and permeability of the SRP at several kilometers depth. Heat transfer in this framework is modeled to give optimal reservoir volumes capable of supporting a functioning geothermal plant.

2. GEOLOGIC SETTING

The SRP is a large volcanic province in the North Western United States formed as the North American Plate traveled SW over a stationary mantle-plume hotspot. Bimodal volcanism cut across the northern Basin and Range creating a large swath of volcanic fields 550 km by 100 km extending from the 16-My McDermitt field in in south western Idaho, north eastern Nevada to the 2-My-to-present Yellowstone Plateau (Morgan and McIntosh, 2005; Brott et al., 1981). Nested caldera structures record time-transgressive younging to the ENE of ignimbrites and lavas created by hot, dry and voluminous silicic volcanism as the plate moved WSW at approximately 3 – 3.5 cm/yr (Shervais et al., 2005; Branney et al., 2007). Erupted volumes of estimated from individual tuff units range from 750 km^3 to >1800 km^3 with individual eruptions estimated at 0.5 km^3 (Morgan and McIntosh, 2005). The consequent tuff deposits have been capped by post-hotspot basalts that have most recently erupted 2 ka (Shervais et al., 2005).

The hotspot model has been disputed in some instances, it remains the most commonly accepted model and has a broad spectrum of supporting evidence including tectonic uplift and subsequent collapse along the track of the hotspot, a large geoid anomaly underneath Yellowstone, seismic tomography, and helium isotopes (Shervais et al., 2005).

Near Twin Falls at ~114˚ longitude, a distinction is made between the western and eastern Snake River Plain (WSRP, ESRP). Whereas the WSRP is a structural graben and measured heat flows are similar to the Basin and Range (Shervais et al., 2013; Blackwell et al., 2010), there is minimal faulting along the margins of the ESRP and heat flows are elevated to ~110 mW/m^2 (Shervais et al., 2005; Blackwell et al., 2010).

Exposures of some of the voluminous silicic volcanics largely reside along the margins of the SRP. Descriptions of and correlations between tuff units document the extreme heterogeneity in rheologic properties between separate flows (Morgan and Doherty, 1984). Features like vitrophyres, lithophysae, and devitrification will influence the hydrologic character of potential reservoirs on the ESRP.

2.1 Examples of Well Logs

Well logs of deep exploration boreholes on the ESRP document heterogeneous stratigraphies (Doherty et al., 1979; Phillips, 2010). Units of rhyolites, tuffs of variable welding, and basalts are often intercalated with fluvial sands, lacustrine mud, eolian sand, and 2 m – 25 m thick loess. Some wells, like INL WO-2, lack sediments. INEL-1 consists of 0 m – 745 m of basalts interbedded with cinders, silt, tuffaceous silt, and tholeittic basalt; from 746 m – 829 m there is slightly altered tuffaceous silt and silty clay; 830 m – 2460 m is predominantly rhyolitic ash flows, each about 3 – 30 m. The flows are altered vitroclastic airfall ashflows, nonwelded ashflows, and reworked tuffaceous sands. The units are often dense and devitrified. Alteration on fracture surfaces consists of calcite, quartz, hematite, pyrite, and clay minerals. From 2461m on, the borehole reaches a dense, hydrothermally altered aphanitic rhyodacite porphyry (Doherty et al., 1979).

Situated in the Huckleberry Ridge Tuff, wells UNST-7 and UNST-8, situated in the Huckleberry Ridge tuff, tap into ~200 m of Huckleberry Ridge Tuff, 50 m of basalt intercalated with sediments of ranging from clay to pebble conglomerates, and >600 m of rhyolite and rhyolite tuff (Phillips, 2010).

3. REGIONAL AND IN-SITU CHARACTERISTICS

3.1 Heat Flow

Heat flow has directly formed many of the modern topographic features on the ESRP. Thermal buoyancy causes increased elevation of the ESRP from west to east and along the axis relative to the margins (Shervais et al., 2005). During eruption of high volumes of silicic magmas, or while calderas are active, there is regional uplift of roughly 2 km. As the heat source shifts eastward in the case of the SRP, the crust thermally contracts and sinks (Brott et al., 1981). Age-elevation models and gravity data support the influence of thermally induced subsidence along the axis and on the margins (Brott et al., 1981)

Upper crust (0 -2 km) temperatures are largely controlled by the extensive - approximately 95 km x 300 km by up to 400 m thick - and fast paced – horizontal flows of ~ 1.6 km/yr - SRP aquifer (Brott et al., 1981; Smith, 2004). Cool aquifer waters control the thermal regime in the Quaternary basalt flows, masking the high heat flow and temperatures of the crust beneath the vadose zone (Podgorney et al., 2013). Bottom hole temperatures at around 3 km can be up to 200˚ C, corresponding to a geothermal gradient of 45-60˚C/km (Podgorney et al., 2013). Heat flow of 110 mW/m^2 below the aquifer is well above values for the Basin and Range region (Brott et al., 1981; Blackwell et al., 2010). It is thought that the high temperatures at relatively shallow crustal depths create conditions amenable to plastic deformation or aseismic creep, thus inhibiting the observable microseismicity.

At great depths, geophysical and geochemical data suggest the presence of a 10 km thick layered mafic intrusion ~12 km below the SRP that would input large amounts of heat into the energy budget of the SRP (Shervais et al., 2006, 2005).

3.2 Stress

Recent GPS surface velocities on the ESRP are thought to show strain rates that are indistinguishable from zero. At $-0.1 \pm 0.4 \times 10^{-9}$ yr^{-1}, ESRP strain rates are an order of magnitude less than in the Basin and Range Province to the northwest, which is extending at $5.6 \pm 0.7 \times 10^{-9}$ yr^{-1} (Payne et al., 2008). While the current stress state is unknown and few studies have attempted to measure in-situ stresses, there is geologic and GPS evidence of the orientation of the stress field and tectonic setting. The discrepancy in plate velocities between the Yellowstone Plateau, which is extending moving at ~ 3 mm yr^{-1}, and the ESRP, which is extending to the southwest at ~ 2.2 mm yr^{-1}, suggests a contemporary compressional tectonic setting and time-dependent deformation on the ESRP (DeNosaquo et al., 2009; Puskas et al., 2007).

Volcanic rift zones (VRZ) trending generally NW on the SRP record extension since ~4 ma. The trends of these VRZs - the Great Rift at N45˚W and Arco-Big Southern Butte at N40˚W - are perpendicular to the least horizontal compression orientation at the time of their formation, indicating a compression-positive σ_3 at ~N45˚E (Kuntz et al., 1992). This general stress orientation is also manifested in cinder cones aligned at ~N42˚E used in the stress map of the coterminous United States (Zoback and Zoback, 1980). Figure 1a shows the locations and orientations of least horizontal compressional stress on the SRP inferred by vent orientations.

Stress magnitudes on the SRP are poorly constrained. One of the few attempts at quantifying the magnitude of stress at depth was performed by *Moos and Barton* (1990) using borehole televiewer data logged from multiple wells at the INEL desert site, including the 3 km deep INEL-1. Due to the absence of borehole breakout over the entire depth, lack of detailed strength measurements for the heterogeneous population of siliceous volcanics, and lack of hydraulic fracturing tests, proper calculations of stress magnitudes were not possible (Moos and Barton, 1990).

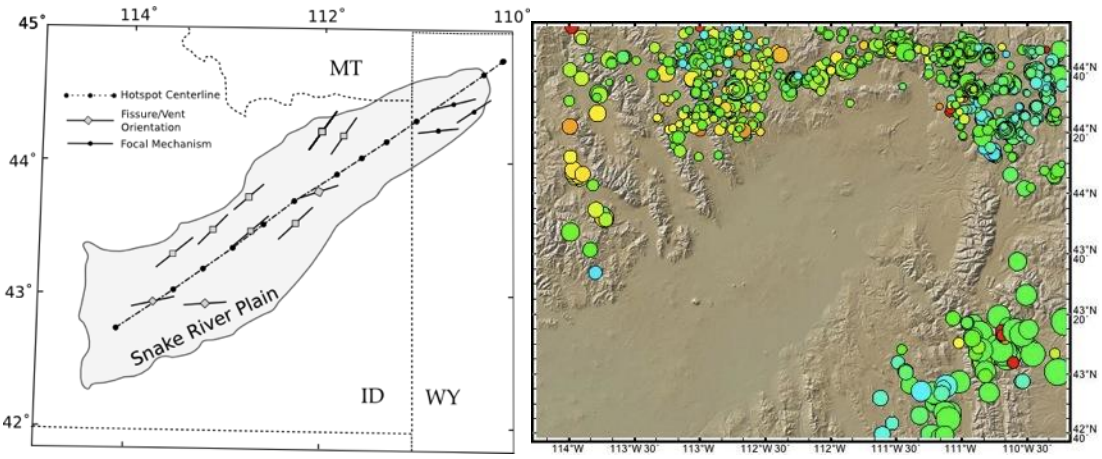

Figure 1: LEFT – Orientation of minimum horizontal compression (S_h) on the SRP inferred from volcanic vents on older portions of the SRP and focal mechanisms near more seismically active zones closer to the YP. RIGHT – earthquake epicenters with circle scaled to magnitude from 2002 to present.

One critical statement about the stress magnitudes is that for there to be no borehole breakout, the vertical stress must be greater than the horizontal stresses, where vertical stress is typically the lithostatic pressure or overburden (Moos and Barton, 1990; Stock et al., 1985). As compressive stress accumulates at the azimuth of the S_h direction to cause the spalling responsible for breakout at approximately three times the magnitude of S_H, there is a high possibility that the horizontal differential stress is rather minimal, or the compressive strengths of the lithologies are greater than the loading. Considering many boreholes on the SRP do not display breakout, such as the recent deep HOTSPOT boreholes and notably the Kimberly well that also breaches into welded tuffs, a low differential stress could characterize more areas than just the INL desert site (Shervais et al., 2013).

The relative aseismicity of the SRP (figure 1b) compared to the surrounding Basin and Range and Yellowstone Plateau can be interpreted as an expression of minimal deviatoric stress and increased strength from the capping of the tuffs by post-hotspot basaltic volcanism (DeNosaquo et al., 2009). Others have attributed this phenomenon as being a result of a migrating or inactive basalt source or from high temperatures allowing aseismic creep in the crust (Brott et al., 1981).

3.3 Permeability and barriers to fluid flow

The traditional paradigm associated with exploitable geothermal systems in the Basin and Range is the association with high strain rates and active deformation (Faulds et al., 2012) that would serve to actively damage any hydrothermal sealing taking place. ESRP cores show that the tuff units that they access are not wanting for secondary permeability features. In deep boreholes at depths reaching welded tuffs, BHTV has logged large populations of fractures evenly distributed over the unit. Sub-horizontal fractures exist, but it is primarily the fractures with wider apertures that tend to strike WSW and dip NNW (Moos and Barton, 1990). The sealing of fractures by precipitation from hydrothermal waters acts to dramatically decrease in-situ permeability in these units, but is evidence of past hydrothermal circulation possibly accompanying caldera collapse. Moos and Barton (1990) also saw a correlation with non-sealed fracture zones and thermal anomalies possibly due to fluid flow in or out of the well.

Smyth and Sharp (2006) have collected laboratory and in-situ hydrologic studies of tuffs primarily conducted at the Nevada Test site at Yucca Mountain. Limited boreholes drilled into the plain reveal a range of nonwelded-to-welded tuff, and tuffaceous interbeds of air-fall and ashflow tuffs that would be expected for caldera complexes (Doherty et al., 1979; Cole et al., 2005b). Hydraulic conductivities determined for silicic volcanics (figure 2) have a maximum value on the order of 10^{-5} m/s, and tend to increase with porosity (LeCain, 2012). Fluid flow in fractured rocks is likely to be focused along younger faults, not in the matrix, and in-situ tests like slug tests and pumping tests give better estimations of holistic hydrologic properties of an aquifer or potential reservoir. These often cover a large range of depths, but can be tuned to find properties of specified units (Smyth and Sharp, 2006).

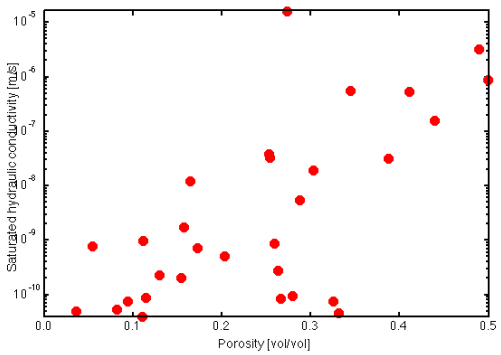

Figure 2: Porosity and saturated hydraulic conductivity of borehole samples at the Yucca Mountain test site, from *LeCain, 2012.*

For EGS purposes in unsaturated heat reservoirs, integrated hydrologic properties of the ESRP tuffs would be a good preliminary estimation for flow. Due to the heterogeneity expressed in variably welded tuffs, hydrologic responses of the reservoir are likely to evolve over time as saturated zones develop. In general, greater degrees of welding in tuffs correlate with higher densities of columnar cooling joints. Fractured zones will preferentially carry fluids, especially in such impermeable matrix. In regards to unwelded tuffs, the high capillary tension of the pores does not inhibit fluid flow by imbibition; rather, fracture skins form and limit the imbibition in time scales useful for reservoir use (Smyth and Sharp, 2006).

After the cessation of volcanic activity associated with caldera formation, large crustal magma bodies on the scale of the width of the postulated SRP calderas will maintain geothermal systems for approximately 2 My (Kolstad and McGetchin, 1978). The ages of ignimbrites in the buried calderas of the ESRP show that the Heise Volcanic Field was active from 6 – 4 mya, thus any residual heat in hydrothermal systems is theoretically depleted; however, studies estimate that for general caldera systems, only 1%-10% of the total thermal energy is in the hydrothermal system. The remaining energy resides in low the permeability matrix and residual magma (Wohletz and Heiken, 1992). Accessing these low permeability zones is essential in EGS development.

3.4 Natural and Induced Fractures

3.4.1 Existing Fracture Systems: From Calderas to Flows

The processes and features associated with rhyolitic caldera formation and collapse are well recognized (Cole et al., 2005a). Intra- and extra caldera facies give insight into what may be encountered in a buried caldera system (Wohletz and Heiken, 1992). Association of active geothermal fields with the permeable regions of the large calderas – i.e. the many productive fields in the Taupo Volcanic Zone in New Zealand and Valles Caldera in New Mexico – indicates the importance of locating these permeable ring fault zones when trying to site a geothermal reservoir. We previously noted that the ring faults are mostly sealed based on evidence from INEL-1 and temperatures observed in boreholes, but enhancing the fracture permeability in these zones might be advantageous.

Figure 3: Stitched photograph of welded Huckleberry Ridge Tuff in Teton Canyon just downstream of the Teton Dam failure site to the NE. Fluid flow in welded tuffs will occur along fracture pathways. Inset is a detail of the outcrop

There is direct evidence of pre-existing joints in outcrops of ESRP-type silicic volcanics at the margins of the plain (figure 3) and beneath the basalts near inferred ring fractures of buried rhyolitic calderas (Moos and Barton, 1990; Shervais et al., 2013). While it is questionable if fracture characteristics and connectivity observed at the surface extrapolate linearly to depth due to changing stresses, there have been efforts to predict effective permeability based on surface fracture maps and studies (Manning and Ingebritsen, 1999; Pollyea and Fairley, 2012). Given the effectively uniform and lithostatic stress on the ESRP, the validity of this model could hold for target geothermal reservoirs in the shallow lithosphere.

On the scale of a single ignimbrite flow, which averages 0.5 km^3 for SRP-YP tuffs, there can be unique structural features and lithologic zonation dependent on depositional and post-depositional deformation history. Emplacement of Huckleberry Ridge Tuff from the Yellowstone Plateau on top of sedimentary diapirs lead to the formation of ~1 m, post- compaction viscous folds, en echelon tensional fractures, and cm to m wide vertical cooling joints occasionally offset by small-scale shears (Geissman et al., 2010; Millard et al., 2005). Embree et al documented and conceptualized these rheomorphic features at the site of the failed Teton Dam near Newdale, ID. Figure 4 shows the zones unique to the Huckleberry Ridge Tuff (Embree et al., 2011).

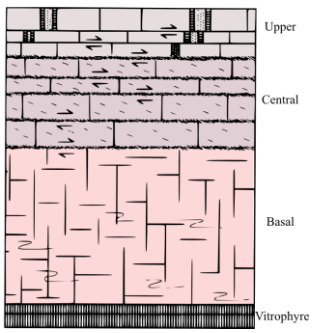

Figure 4: Schematic drawing of the structural and lithologic zoning exposed in outcrops of Huckleberry Ridge Tuff in Teton Canyon. From *Embree et al., 2011*.

3.4.2 Induced Fractures

Accessing adequate matrix surface area for heat exchange in the subsurface of the ESRP requires require reservoir stimulation in order to enhance the conductivity of natural fractures that have been sealed by precipitation of minerals from hydrothermal fluids. Tensile fractures noted in the HOTSPOT Kimberly well have been noted at depth, possible from the influence of cool drilling fluids creating thermal stresses in the hotter ignimbrites (Shervais et al., 2013). Hydraulic hydraulic fracturing tests are known to constrain the magnitude of S_h, or minimum confining stress (Hickman and Zoback, 1983). The direction of the tensile fracture is controlled by the remote stress and forms parallel to the maximum compressive stress direction, or S_H. This is the same reason that vents are perpendicular to the minimal compressive stress.

Around a pressurized borehole, orientations of the principal stress directions are going to be influenced both by fluid pressure and the remote stress. Increasing fluid pressure in the borehole will increase the radius of influence of the borehole perturbations. Figure 5 shows the effects of heightened fluid pressure and the trace of potential mode I tensile fractures.

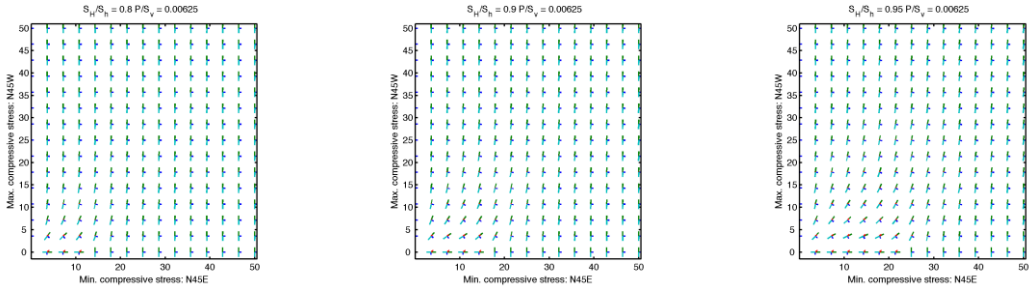

Figure 5: Stress field perturbations due to a pressurized borehole under increasing lithostatic conditions (from left to right). Short and long tick marks are the local S_h and S_H, respectively. Tensile fractures will parallel the direction of S_H.

3.4.3 Fracture Propagation

Modeling the extent of fracture propagation in a homogeneous isotropic material is a difficult and problematic undertaking. Extending this goal to predicting the formation of hydraulic fractures in the heterogeneous and poorly constrained stratigraphy of the ESRP is accompanied with added difficulty and uncertainty.

Locating a host fault for earthquakes based on their generated seismic cloud has been shown to be feasible for the initial shock, aftershock, and magma intrusion-induced earthquakes, the latter of which has been resolved onto several discrete fracture surfaces (Carena et al., 2002; Carmona et al., 2010). Recently, microseismics produced by pressure diffusion into a large fractured rock mass (several km^2) near a dam have been used to delineate the location and orientation of several fractures within 10 m for a majority of inferred surfaces (Pytharouli et al., 2011). Such a method would prove invaluable for constraining the distributions of fracture systems in rhyolites as it is generally non-invasive and there are pre-existing wells that could be used to induce seismicity.

4. HEAT EXTRACTION MODELING

Analytical solutions to heat extraction processes – i.e. (Carslaw & Jaeger, 1959)– are widely used in reporting geothermal potential and for thermal drawdown of the reservoir (Tester et al., 2006; Axelsson et al., 2001). These models are single fracture solutions that assume cooling fronts do not interact between two or more fractures with advecting fluids transporting heat, thereby underestimating the efficiency of extraction and geothermal potential of a potential site. Reservoirs are likely to be more densely fractured than one isolated fracture, necessitating the use of more complex mathematical treatments. These types of solutions are not readily accomplished and involve semi-analytical particular solutions requiring numerical Laplace transforms.

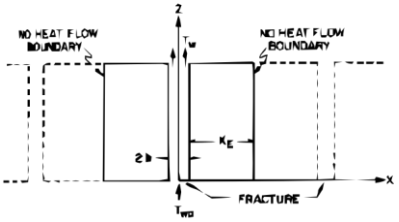

Figure 6: Conceptual model utilized by Gringarten et al. (1975). *b* is the fracture aperture, x_e is the fracture half spacing, and water flows through fractures in the z-direction. Model is applied per unit thickness of the reservoir in this paper.

Gringarten et al. (1975) solved the extraction of thermal energy from a rock matrix with *n* interacting cooling fronts, conceptualized in figure 6. The 2D advection-diffusion model is semi-analytical and is solved with a numerical Laplace inversion code in MATLAB for the purposes of this paper. Outlet water temperature, T_{wd}, is expressed in Laplace space as

$$T_{wd}(z_D, s) = \frac{1}{s}\exp(-z_D s^{1/2}\tanh(\frac{r_w c_w Q x_e}{2K_R H})s^{1/2}) \quad \text{(eq. 1)}$$

where ρ_w is the density of water [kg/m^3], c_w is the specific heat of water [J/K], Q is volumetric flow rate per fracture per unit length in the y-direction [m^2/s], x_e is fracture spacing, K_R is the thermal conductivity of the rock [W/m^{2}K], H is an arbitrary length, and s is a Laplace parameter. The geothermal gradient is neglected on the scale of a geothermal reservoir, and thermal properties of the rock and water are constant. Reservoir parameters include flowpath length, fracture spacing, fracture aperture, number of fractures, and intial reservoir temperature. Production dictated parameters are mean velocity and fluid injection temperature.

Pragmatic reasons dictate minimizing reservoir volume while maximizing enthalpy. In applying the model to a hypothetical EGS site on the ESRP, production targets are set at Q = 0.063 m^3/s (1000 gpm) for 20 years. Initial reservoir temperature is 150˚ C to 200˚C. To optimize for a minimal reservoir volume, uniformly distributed random shape parameters (fracture spacing and flowpath length) are applied to the Gringarten solution. Following is an example of using the Gringarten solution for estimating thermal power extracted from a hypothetical reservoir (tables 1 & 2, figure 7).

In general, overlapping cooling fronts increase the rate of heat extraction and cool the reservoir more quickly; this is demonstrated in figure. Outlet water temperature and thus thermal power increases as fracture spacing increases until the curve levels off at some distance controlled by the thermal properties of the reservoir rock and the flow rate through the fractures.

Calculations are per unit height of the aquifer, making these underestimations for the extractable energy available for a given footprint of the reservoir. We assume that water is injected in one well and produced at another (dipole), thus not taking into account losses through the fracture network or other configuration of production and injection wells. Though highly idealized, this heat transfer model is readily accomplished in an environment like MATLAB and could be crafted into a standalone open source product to distribute for educational and preliminary feasibility purposes. The extent of non-uniqueness is not explored in this paper, but the MATLAB script allows many reservoir geometries and parameters to be explored quickly enabling the user to see patterns between sets of parameters.

Q (m^3/s)	*T_{res} (˚C)*	*T_{inj} (˚C)*	*Aperture (mm)*	*Fracture Spacing (m)*	*Flowpath length (km)*	*# of fractures*	*Production time (yrs)*
0.063	150, 200	30	1	0 - 1000	0 - 2	10	20

Table 1: Parameters used for minimizing the volume of a hypothetical reservoir in welded rhyolitic tuff.

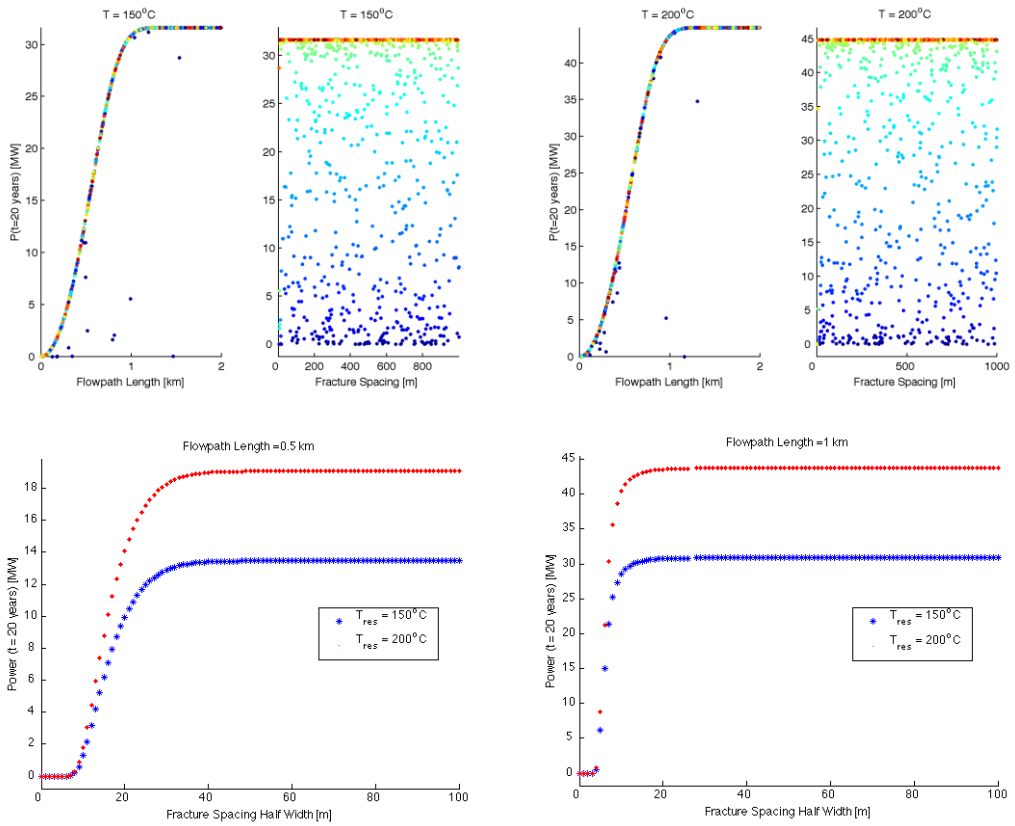

Figure 7: Thermal power extracted from reservoir after 20 years of production. TOP – Dots show the thermal power for a random configuration of distance between injection and production wells and distance between fractures from a 150˚C (left) and 200˚C (right) reservoir. BOTTOM – Effect of fracture spacing on thermal power for 500 m and 1000 m flow paths.

	Reservoir Temperature (˚C)			
	150		**200**	
Flowpath length (km)	0.5	1	0.5	1
Fracture ½ spacing (m)	40	20	40	20
Thermal Power Output (MW)	13	30	19	43
Area (km^2)	0.4	0.4	0.4	0.4
MW/km^2	**32.5**	**75**	**47.5**	**107.5**

Table 2: Selections of ideal reservoir geometries selected from randomly distributed length and spacing pairs with corresponding thermal power estimated using the Gringarten solution.

5. DISCUSSION AND CONCLUSION

Calderas inherently host large amounts of energy in low permeability, intra-caldera rocks that were not host to large movements of fluids over the course of formation and collapse (Wohletz and Heiken, 1992). Conduction of heat is the dominate heat transfer mechanism and could be accessed using EGS; however, it might be advantageous to situate potential EGS sites near ring faults and induce fractures into these faults. The sealed faults could be more likely to reinitiate, as they are previous planes of weakness.

New methods using microseismic monitoring for detailed characterization of fracture surfaces will prove to be invaluable for detecting natural fractures and the extent of hydraulic fracturing. Spatial knowledge of fractures in a reservoir can then be used in a model like the Gringarten model to estimate the total energy that can be extracted from that reservoir geometry.

Calderas are very complex systems and we should be aware of the limitations of any modeling of fluid flow or resource potential before we have better constraints on lithologies and stress. Ideas presented here offer some way to get first order estimates of the potential available resources. More in-situ and laboratory testing of stress magnitudes, hydrologic properties, heat flow, and mechanical properties will be helpful in understanding how injection into the SRP tuffs and rhyolites will proceed.

ACKNOWLEDGEMENTS

This work is supported by a Center for Advanced Energy Studies (CAES) LDRD Grant 13-068. We also would like to thank Rob Podgorney, Jerry Fairley, and Matt Pendleton.

REFERENCES

Axelsson, G., Flovenz, O.G., Hauksdottir, S., Hjartarson, A., and Liu, J., 2001, Analysis of tracer test data, and injection-induced cooling, in the Laugaland geothermal field, N-Iceland: Geothermics, v. 30, p. 697–725, doi: 10.1016/S0375-6505(01)00026-8.

Blackwell, D., Stepp, P., and Richards, M., 2010, Comparison and Discussion of the 6 Km Temperature Maps of the Western US Prepared by the SMU Geothermal Lab and the USGS, *in* GRC Transactions, p. 515–520.

Branney, M.J., Bonnichsen, B., Andrews, G.D.M., Ellis, B., Barry, T.L., and McCurry, M., 2007, "Snake River (SR)-type" volcanism at the Yellowstone hotspot track: distinctive products from unusual, high-temperature silicic super-eruptions: Bulletin of Volcanology, v. 70, p. 293–314, doi: 10.1007/s00445-007-0140-7.

Brott, A., Blackwell, D.D., and Ziagos, J.P., 1981, Thermal and Tectonic Implications of Heat Flow in the Eastern Snake River Plain: Journal of Geophysical Research, v. 86, p. 11,709–11,734.

Carslaw, H.S., and Jaeger, J.C., 1959, Conduction of heat in solids.pdf: London, Oxford University Press.

Cole, J.W., Milner, D.M., and Spinks, K.D., 2005a, Calderas and caldera structures : a review: Earth Science Reviews, v. 69, p. 1–26, doi: 10.1016/j.earscirev.2004.06.004.

Cole, J., Milner, D., and Spinks, K., 2005b, Calderas and caldera structures: a review: Earth-Science Reviews, v. 69, p. 1–26, doi: 10.1016/j.earscirev.2004.06.004.

DeNosaquo, K.R., Smith, R.B., and Lowry, A.R., 2009, Density and lithospheric strength models of the Yellowstone–Snake River Plain volcanic system from gravity and heat flow data: Journal of Volcanology and Geothermal Research, v. 188, p. 108–127, doi: 10.1016/j.jvolgeores.2009.08.006.

Doherty, D., McBroome, L., and Kuntz, M., 1979, Preliminary geological interpretation and lithologic log of the exploratory geothermal test well (INEL-1):.

Embree, G.F., Phillips, W.M., Champion, D., Moore, D.K., Jordan, B.R., and Geissman, J.W., 2011, Large-Scale Rheomorphic Structures and Basalt Stratigraphy of the Newdale and Linderman Dam 7 . 5-minute Quadrangles , Eastern Snake River Plain , Idaho, *in* GSA Annual Meeting,.

Faulds, J.E., Hinz, N., Kreemer, C., and Coolbaugh, M., 2012, Regional Patterns of Geothermal Activity in the Great Basin Region , Western USA : Correlation With Strain Rates Distribution of Geothermal Fields: v. 36.

Geissman, J.W., Holm, D., Harlan, S.S., and Embree, G.F., 2010, Rapid, high-temperature formation of large-scale rheomorphic structures in the 2.06 Ma Huckleberry Ridge Tuff, Idaho, USA: Geology, v. 38, p. 263–266, doi: 10.1130/G30492.1.

Hickman,S., and Zoback, M.D.: The interpretation of hydraulic fracturing pressure-time data for in-situ stress determination, in *Hydraulic Fracturing Measurements*, edited by M.D. Zoback and B.C. Haimson, National Academy Press, Washington, D.C., p.44-54 (1983).

Kolstad, C.D., and McGetchin, T.R., 1978, Thermal Evolution Models for the Valles Caldera with reference to a hot dry rock geothermal experiment: Journal of Volcanology and Geothermal Research, v. 3, p. 197–218.

LeCain, G.D., and Stuckless, J.S., Hydrology of the unsaturated zone, Yucca Mountain, Nevada, in *Hydrology and Geochemistry of Yucca Mountain and Vicinity, Southern Nevada and California*, edited by J.S. Stuckless, GSA Memoir 209, p. 9- 72, (2012).

Manning, C., and Ingebritsen, S.: Permeability of the continental crust: Implications of geothermal data and metamorphic analysis, *Rev. Geophys.*, **37**, 127-150 (1999).

Millard, M.A., Clayton, R.W., and Painter, C.S., 2005, Preferred fracture orientations resulting from secondary deformation of a rhyolitic ash flow tuff: 2 Ma Huckleberry Ridge Tuff, Southeast Idaho, *in* GSA Annual Meeting, Salt Lake City, p. 91954.

Moos, D. and Barton, C.A.: In-situ stress and natural fracturing at the INEL site, Idaho, DOE Report EGG-NPR-10631, (1990).

Morgan, L.A., and Doherty, D.J., 1984, Tuff of Blue Creek Elkhorn c , f Tuff of Blacktail: v. 89, p. 8665–8678.

Morgan, L. a., and McIntosh, W.C., 2005, Timing and development of the Heise volcanic field, Snake River Plain, Idaho, western USA: Geological Society of America Bulletin, v. 117, p. 288, doi: 10.1130/B25519.1.

Payne, S.J., McCaffrey, R., and King, R.W., 2008, Strain rates and contemporary deformation in the Snake River Plain and surrounding Basin and Range from GPS and seismicity: Geology, v. 36, p. 647, doi: 10.1130/G25039A.1.

Phillips, W.M., 2010, Well Logs for the Union Oil UNST-7 and UNST-8 Geothermal Test Wells , Newdale 7 . 5-Minute Quadrangle , Idaho Well Logs for the Union Oil UNST-7 and UNST-8 Geothermal Test Wells , Newdale 7 . 5-Minute Quadrangle , Idaho:.

Pierce, K.L., and Morgan, L.A., The track of the Yellowstone hotspot: Volcanism, faulting, and uplift, in *Regional Geology of Eastern Idaho and Western Wyoming*, edited by P.K. Link, M.A. Kuntz and L.B. Platt, GSA Memoir 179, p. 1 – 53, (1992).

Podgorney, R., Mccurry, M., Wood, T., Mcling, T., Ghassemi, A., Welhan, J., Mines, G., Plummer, M., Moore, J., Fairley, J., and Wood, R., 2013, Enhanced Geothermal System Potential for Sites on the Eastern Snake River Plain , Idaho: v. 37.

Pollyea, R.M., and Fairley, J.P., 2012, Implications of spatial reservoir uncertainty for CO2 sequestration in the east Snake River Plain, Idaho (USA): Hydrogeology Journal, v. 20, p. 689–699, doi: 10.1007/s10040-012-0847-1.

Puskas, C.M., Smith, R.B., Meertens, C.M., and Chang, W.L., 2007, Crustal deformation of the Yellowstone–Snake River Plain volcano-tectonic system: Campaign and continuous GPS observations, 1987–2004: Journal of Geophysical Research, v. 112, p. B03401, doi: 10.1029/2006JB004325.

Pytharouli, S.I., Lunn, R.J., Shipton, Z.K., Kirkpatrick, J.D., and do Nascimento, A.F., 2011, Microseismicity illuminates open fractures in the shallow crust: Geophysical Research Letters, v. 38, p. n/a–n/a, doi: 10.1029/2010GL045875.

Shervais, J.W., Kauffman, J.D., Gillerman, V.S., Othberg, K.L., Vetter, S.K., Hobson, V.R., Cooke, M.F., Matthews, S.H., and Hanan, B.B., 2005, Basaltic volcanism of the central and western Snake River Plain : A guide to fi eld relations between Twin Falls and Mountain Home , Idaho: v. 006, doi: 10.1130/2005.fl.

Shervais, J.W., Schmitt, D.R., Nielson, D., Evans, J.P., Christiansen, E.H., Morgan, L., Shanks, W.C.P., Prokopenko, A. a., Lachmar, T., Liberty, L.M., Blackwell, D.D., Glen, J.M., Champion, D., Potter, K.E., et al., 2013, First Results from HOTSPOT: The Snake River Plain Scientific Drilling Project: Scientific Drilling,, p. 36–45, doi: 10.2204/iodp.sd.15.06.2013.

Shervais, J.W., Vetter, S.K., and Hanan, B.B., 2006, Layered mafic sill complex beneath the eastern Snake River Plain: Evidence from cyclic geochemical variations in basalt: Geology, v. 34, p. 365, doi: 10.1130/G22226.1.

Smyth, R.C., and Sharp, J.M. Jr.: The hydrologiy of tuffs, in *Tuffs: Their properties, uses, hydrology, and resources*, edited by G. Heiken, GSA Special Paper 408, Boulder, CO., p. 91- 111. (2006).

Smith, R.P., 2004, Geologic Setting of the Snake River Plain Aquifer and Vadose Zone: Vadose Zone Journal, v. 3, p. 47–58, doi: 10.2113/3.1.47.

Stock, J.M., Healy, J.H., Hickman, S.H., and Zoback, M.D., 1985, Hydraulic fracturing stress measurements at Yucca Mountain, Nevada, and relationship to the regional stress field: Journal of Geophysical Research, v. 90, p. 8691, doi: 10.1029/JB090iB10p08691.

Tester, J.W., Anderson, B.J., Batchelor, A.S., Blackwell, D.D., DiPippo, R., Drake, E.M., Garnish, J., Livesay, B., Moore, M.C., Nichols, K., Petty, S., Toksoz, M.N., and Veatch, R.W.J., 2006, The Future of Geothermal Energy: Impact of Enhanced Geothermal Systems on the United States in the 21st Century:.

Wohletz, K. and Heiken, G.: *Volcanology and Geothermal Energy*, University of California Press (1992).

Zoback, M. Lou, and Zoback, M., 1980, State of Stress in the Conterminous United States: Journal of Geophysical Research, v. 85, p. 6113–6156.